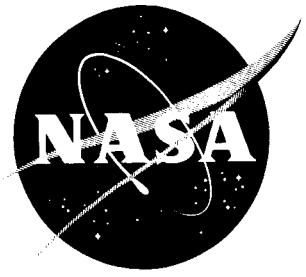

TECHNICAL MEMORANDUM

X-142

AN EXPLORATORY INVESTIGATION

OF THE LOW-SPEED AERODYNAMIC CHARACTERISTICS OF

VARIABLE-WING-SWEEP AIRPLANE CONFIGURATIONS

By William J. Alford, Jr., and
William P. Henderson

Langley Research Center
Langley Field, Va.

NATIONAL AERONAUTICS AND SPACE ADMINISTRATION

WASHINGTON

September 1959

NATIONAL AERONAUTICS AND SPACE ADMINISTRATION

TECHNICAL MEMORANDUM X-142

AN EXPLORATORY INVESTIGATION OF THE LOW-SPEED AERODYNAMIC CHARACTERISTICS OF VARIABLE-WING-SWEEP AIRPLANE CONFIGURATIONS*

By William J. Alford, Jr., and
William P. Henderson

SUMMARY

24100

Wind-tunnel studies at low speeds on four variable-wing-sweep airplane configurations indicated that the final arrangement, which was designed from information obtained on the first three, was longitudinally stable for all sweep angles above 12.5° and directionally stable for all sweep angles and lift coefficients investigated with the maximum static margin only about 9.5 percent of the mean aerodynamic chord $\bar{c}$; thereby the need for wing translation was eliminated. Pitch control provided by the horizontal tail was large and was essentially invariant with either sweep angle or lift coefficient. The results of roll control effectiveness tests indicated that control provided by differential deflections of the horizontal tail looked more attractive than control provided by wing-tip ailerons although the favorable yawing moments due to roll control (by tails) might be excessive.

AUTHOR

INTRODUCTION

An airplane combining supersonic cruise capability with good low-speed capabilities would be useful in many operations. For instance, to strike targets defended by radar and missiles, such an aircraft armed with nuclear warheads could take off from relatively small unimproved air fields, make a supersonic cruise at high altitude to within several hundred miles of the target, and then make its attack from tree-top level at high subsonic speed by utilizing high wing sweep to minimize gust loads. For use as a naval-combat-air-patrol aircraft, desirable carrier operating characteristics and the ability to loiter would be combined with the ability to accelerate to supersonic speed and to intercept an attacking aircraft

*Title, Unclassified.

at a considerable distance from the task force. For use as a supersonic transport, such an aircraft could employ a subsonic climb-out and thus avoid the supersonic "bang" in the neighborhood of crowded metropolitan areas.

In general, the requirements for efficient low-speed and supersonic flight are not compatible. In order to accomplish such a split mission, it becomes necessary either to compromise performance or to alter the configuration in flight. A promising method of such an alteration was demonstrated by the Bell X-5 research airplane program (ref. 1) in which the entire wing semispan was swept and translated. It would be desirable, however, to retain the variable sweep while eliminating the need for wing translation thereby reducing the mechanical complexity, weight, and performance penalties encountered with the X-5. One possible method would be to provide a fixed lifting area ahead of the center of gravity such as a canard surface or a fixed portion of the wing. The destabilizing contribution of these surfaces for a given total lift coefficient would increase with increasing wing sweep (due to loss in lift-curve slope) thereby tending to counteract the effect of the rearward rotation of the wing panels with increasing sweep.

The purpose of this paper is to present a brief description of some of the low-speed aerodynamic characteristics of four variable-wing-sweep-airplane configurations of this type. The first three configurations were exploratory in nature whereas the fourth configuration was developed from knowledge gained from the others. All four were tested at $M = 0.25$ in the Langley high-speed 7- by 10-foot tunnel with the wing outboard panels at various angles of sweep. With the wing of the fourth configuration at 75° of sweep, the speed range was extended to the high subsonic and transonic regions in the Langley 8-foot transonic pressure tunnel and to $M = 2.01$ in the Langley 4- by 4-foot supersonic pressure tunnel. The results of tests made at $M = 2.01$ have been reported in reference 2.

COEFFICIENTS AND SYMBOLS

The results are referred to the body axis system except the lift and drag which, of course, are referred to the wind axis system. All coefficients are nondimensionalized with respect to the geometric characteristics associated with the maximum sweep condition. The moment-center locations are noted on the model drawings.

C_L lift coefficient, $\frac{\text{Lift}}{qS}$

C_D drag coefficient, $\frac{\text{Drag}}{qS}$

C_m pitching-moment coefficient, $\frac{\text{Pitching moment}}{qS\bar{c}}$

C_l rolling-moment coefficient, $\frac{\text{Rolling moment}}{qSb}$

C_n yawing-moment coefficient, $\frac{\text{Yawing moment}}{qSb}$

q dynamic pressure, lb/sq ft

S wing area, sq ft

$\bar{c}$ mean aerodynamic chord, ft

b wing span, ft

α angle of attack, deg

β angle of sideslip, deg

Λ wing leading-edge sweep angle, deg

δ control deflection or dihedral angle, deg

C_{m_δ} pitch control effectiveness parameter, per deg

C_{l_δ} roll control effectiveness parameter, per deg

C_{n_δ} yawing-moment effectiveness parameter due to roll control, per deg

$C_{l_\beta} = \frac{\partial C_l}{\partial \beta}$, per deg

$C_{n_\beta} = \frac{\partial C_n}{\partial \beta}$, per deg

C_{L_α} lift-curve slope, per deg

$(L/D)_{max}$ maximum lift-drag ratio

Subscripts:

A	refers to auxiliary horizontal tail of configuration II
T	refers to horizontal tail of configuration III
o	refers to zero lift condition

MODELS AND APPARATUS

Configuration I, shown in figures 1 and 2, was essentially an arrow wing with movable outer wing panels whose leading-edge sweep angle could be varied from 0° to 80° (similar to the British "Swallow" design). The inner wing panel was fixed at $\Lambda = 80°$. The panel pivot point was located at 34 percent of the wing semispan for $\Lambda = 80°$. The wing employed NACA 63_{10}A014 airfoil sections normal to the leading edge. The wing was fixed, with zero dihedral and incidence, to the center line of an ogive-cylinder body of the minimum size possible to house the six-component strain-gage balance. Control for this configuration was to be obtained from deflections of the four-engine nacelles (one over and one under each wing semispan). These nacelles were constructed of aluminum tubing and were mounted on pylons in such a manner that deflections could be obtained in the longitudinal planes for pitch or roll control and in the lateral plane for directional control. The pylons also pivoted so that they could be alined in the free-stream direction for the various wing sweep angles.

A drawing and photographs of configuration II, which was a canard arrangement, are presented in figures 3 and 4, respectively. The outer wing panels had sweep angles of 0°, 25°, 50°, 62.5°, and 75°. The inner wing panel was fixed at $\Lambda = 75°$. The pivot point was located at 28 percent of the wing semispan for $\Lambda = 75°$. The wing employed NACA 63_8A007.7 airfoil sections normal to the leading edge. The wing was fixed, with zero dihedral and incidence, to the center line of a fuselage which had a flat top and bottom and semicircular sides. The fuselage nose employed ogival plan-form and side-view contours. Pitch control for this arrangement was obtained by deflection of the canard surface. A folding auxiliary tail was employed to provide longitudinal stability for $\Lambda = 0°$ and to provide additional directional stability for the high-speed condition with the 75° wing.

Configuration III, the details of which are presented in figures 5 and 6, had a conventional rearward-tail arrangement (for the unswept condition). The fuselage and the wing were the same as those employed in configuration II except that the wing was moved forward on the fuselage.

The all-movable horizontal tail, which provided pitch control for the unswept condition, folded down to -90° dihedral for $\Lambda = 75°$ to provide additional directional stability. For this maximum-sweep condition, elevons located on the wing were employed for pitch control.

A drawing of configuration IV is presented in figure 7, and a photograph is presented in figure 8. The pivot point for the outer wing panels was located at approximately 56 percent of the semispan of the wing at $\Lambda = 75°$. The wing panels had sweep angles of 12.5°, 25°, 50°, 62.5°, and 75°. The inboard panel was fixed at $\Lambda = 60°$. The wing employed NACA 636A004.5 airfoil sections normal to the leading edge. The horizontal and vertical tail panels were identical in plan form. The all-movable horizontal tail, which was used for pitch control, was mounted on the body center line at -15° dihedral. Roll control could be provided by ailerons located at the wing tips or by differential deflection of the horizontal tail panels.

All models were internally instrumented with six-component strain-gage balances and were sting mounted as shown in the model photographs.

TESTS, CORRECTIONS, AND ACCURACY

The tests were conducted in the Langley high-speed 7- by 10-foot tunnel with free transition at a Mach number of 0.25 which corresponds to a Reynolds number of 1.5×10^6 per foot.

Jet-boundary corrections calculated by the method of reference 3 have been applied to the drag and angle of attack. Blockage corrections applied to dynamic pressure were calculated by the method of reference 4. The base pressure was measured and the data corrected to a base pressure equal to free-stream static pressure. The angles of attack and sideslip were corrected for the deflection of the sting and balance under load.

The estimated accuracy of the measured quantities under load is as follows:

C_L	±0.009
C_D	0.0025
C_m	0.0010
C_l	0.0003
C_n	0.0004
α, deg	±0.1
β, deg	±0.1

PRESENTATION OF RESULTS

A summary of the aerodynamic characteristics for each of the various configurations is presented in the following figures:

Configuration	Figure
I	9
II	10
III	11
IV	12 and 13

DISCUSSION

Configuration I

The variation of pitching-moment coefficient with lift coefficient for configuration I (fig. 9) indicates that severe nonlinearities are present for moderate lift coefficients, the lift coefficient associated with the onset of instability decreasing as the wing sweep angle is increased. The longitudinal stability level, or static margin, as shown by the difference between the neutral point $\left(\frac{\partial C_m}{\partial C_L}\right)_{C_L \approx 0}$ and the estimated center-of-gravity location in percent $\bar{c}$ is satisfactory and is of the order of 9 percent up to approximately the 50° leading-edge-sweep point with instability indicated for sweep angles greater than 60°. This estimated center-of-gravity location accounts for the estimated engine, fuel, and structural weights. It should be noted that in order to have this configuration stable at the high sweep angles the center of gravity would have to be located farther forward than would appear to be practical. Directional stability was obtained for all sweep angles between 20° and 80°. The large increase in C_{n_β} associated with $\Lambda = 80°$ is due to the increase in moment arm of the nacelle supporting pylons which are the only lifting surfaces that contribute to the directional stability. The pitch-control-effectiveness parameter C_{m_δ} obtained by deflecting

the nacelles with the power off is trivial. Although not shown here, slightly better directional control, particularly for the higher wing sweeps, was obtained inasmuch as the nacelle pylons also pivoted.

Configuration II

Although instabilities are still in evidence, the pitch characteristics of configuration II (fig. 10) are less abrupt than those of configuration I. This second configuration is longitudinally stable up to approximately 70° of sweep although the static margin appears excessive for the intermediate sweep range. The results of tests made throughout the sweep range with the auxiliary tail folded ($\delta_A = 90°$) and unfolded ($\delta_A = 0°$) indicated that it was relatively ineffective because it was closely coupled with the wing and therefore in a region of high downwash rate. The directional stability parameter C_{n_β} is initially increased by having the auxiliary tail folded although, for this condition, instability occurs at a lower lift coefficient. The rather abrupt decrease in C_{n_β} for both sweep angles is presumed to be due to the combination of the canard-surface and body vortices producing adverse flow angularities on the vertical tail. The reason for the earlier decrease for the high sweep condition is due to the fact that higher values of α are required for a given value of C_L. The longitudinal control effectiveness parameter C_{m_δ} becomes zero at a lift coefficient of 0.7 due to canard-surface stall.

Configuration III

The results for configuration III in figure 11 indicate that the pitching-moment characteristics are considerably better than those of configurations I and II in that the curves are considerably more linear and the lift coefficients for the tendency toward instability are increased. This configuration was found to be stable throughout the entire sweep range investigated although the static margin for sweep angles near 50° sweep again appears excessive. This excessive static margin is the result of having the pivot point located too far inboard on the wing span which results in a large portion of the wing area being movable. Folding the horizontal tail decreased the static margin approximately 5 percent. This configuration was directionally stable to large lift coefficients with $\Lambda = 0°$ and this stability was increased considerably for the $\Lambda = 75°$ condition and with the horizontal tail folded 90°. Since the horizontal tail was folded for $\Lambda = 75°$, elevons were used for pitch control. These proved to be ineffective. For $\Lambda = 0°$ control provided by the horizontal tail was large and essentially constant throughout the lift-coefficient range investigated.

[redacted]

Configuration IV

A survey of the information obtained on the first three configurations indicated that considerable reduction in the neutral-point variation could be obtained by increasing the lift capability of the fixed portion of the wing ahead of the center of gravity. This was done by moving the wing forward relative to the center of gravity, reducing the sweep of the fixed portion, and moving the pivot outboard. The slight reduction of aspect ratio in the landing configuration due to the more outboard pivot is of little significance in this aspect-ratio range. The results obtained for configuration IV (fig. 12) which employed such a modification, indicates that the configuration is longitudinally stable for all sweep angles above 12.5°. The variation of pitching-moment coefficient with lift coefficient indicates a tendency toward instability at the higher lifts. Comparisons with contemporary airplane configurations indicate that these characteristics should be satisfactory. The maximum static margin occurs at a sweep angle of approximately 50° and is about 9.5 percent of $\bar{c}$ which is about one-half that associated with either configuration I or II (figs. 10 and 11). It should be noted that the static margins of configuration IV (fig. 12) at 25° sweep (which is considered a practical margin) and at 75° sweep are within 2.5 percent $\bar{c}$ of each other.

L
6
8
4

The pitch control effectiveness parameter C_{m_δ} for configuration IV associated with the all-movable horizontal tail appears to be adequate and is essentially invariant with either wing-sweep angle or lift coefficient for the ranges investigated. The lift-curve slope increases from approximately 0.045 to 0.088 as the wing sweep angle is reduced from 75° to 12.5° and the $(L/D)_{max}$ increases from 7.1 to 10.8 for the same sweep reduction. The configuration is directionally stable throughout the sweep range and C_{n_β} decreases only slightly for the highest lift investigated. As would be expected, the effective dihedral parameter C_{l_β} at low lift coefficients is increased as the sweep was increased from $\Lambda = 12.5°$ to $\Lambda = 75°$.

The results of tests made to determine the lateral control characteristics of both ailerons and differential deflections of the horizontal tail panels for configuration IV are presented in figure 13. These results show that the aileron provided large values of the control effectiveness C_{l_δ} for the minimum sweep condition although a rather severe reduction was evident with increasing angle of attack. For $\Lambda = 75°$, the aileron became relatively ineffective. The use of differential deflections of the horizontal tail panels for roll control provided levels that were estimated to be acceptable and which increase somewhat with increasing angle of attack. The yawing moments due to roll control C_{n_δ}

are adverse for the aileron and are favorable, although possibly excessive, for the tail control.

CONCLUDING REMARKS

Investigations made at low speed to determine the aerodynamic characteristics of four variable-wing-sweep airplane configurations indicated that for the first configuration, which was an arrow wing, an adequate static margin existed up to a sweep angle of 55°, and directional stability existed that increased with wing-sweep angle. Pitch control provided by deflecting engine nacelles with the power off was trivial. Configuration II, which was a canard arrangement, was longitudinally stable up to 70° of wing sweep but had excessive static margin for the intermediate sweep angles. Pitch control provided by the canard and the directional stability became zero at moderate lift coefficients. Configuration III, which was a conventional rearward-tail arrangement, was longitudinally stable throughout the wing sweep angle range (0° to 75°) although excessive static margins existed near a sweep angle of 50°. Elevons used for pitch control for the maximum sweep were ineffective although control provided by the horizontal tail was large for the unswept condition. This configuration was directionally stable for all sweep angles to high-lift coefficients.

The final arrangement, configuration IV, which was a rearward-tail arrangement designed from information obtained on the first three configurations, was longitudinally stable for all sweep angles above 12.5° and directionally stable for all sweep angles and lift coefficients investigated. The maximum static margin was only about 9.5 percent of the mean aerodynamic chord; thereby the need for wing translation was eliminated and the accompanying complexity, weight, and performance penalities were avoided. Pitch control provided by the horizontal tail was large and essentially invariant with either sweep angle or lift coefficient. Roll control by differential deflections of the horizontal tail looked more promising than did roll control provided by wing-tip ailerons although the favorable yawing moments due to roll control by the tail might be excessive. In general, this configuration exhibited the possibility of combining good high-speed and low-speed characteristics into one airplane requiring variable sweep in only the outboard wing panel with no translation needed.

Langley Research Center,
National Aeronautics and Space Administration,
Langley Field, Va., July 29, 1959.

L 6 8 4

[redacted]

[redacted]

REFERENCES

1. Kemp, William B., Jr., Becht, Robert E., and Few, Albert G., Jr.: Stability and Control Characteristics at Low Speed of a 1/4-Scale Bell X-5 Airplane Model. Longitudinal Stability and Control. NACA RM L9K08, 1950.

2. Spearman, M. Leroy, and Foster, Gerald V.: Stability and Control Characteristics at a Mach Number of 2.01 of a Variable-Wing-Sweep Configuration With Outboard Panels Swept Back 75°. NASA TM X-32, 1959.

3. Gillis, Clarence L., Polhamus, Edward C, and Gray, Joseph L., Jr.: Charts for Determining Jet-Boundary Corrections for Complete Models in 7- by 10-Foot Closed Rectangular Wind Tunnels. NACA WR L-123, 1945. (Formerly NACA ARR L5G31.)

4. Herriot, John G.: Blockage Corrections for Three-Dimensional-Flow Closed-Throat Wind Tunnels, With Consideration of the Effect of Compressibility. NACA Rep. 955, 1950. (Supersedes NACA RM A7B28.)

L 6 8 4

[redacted]

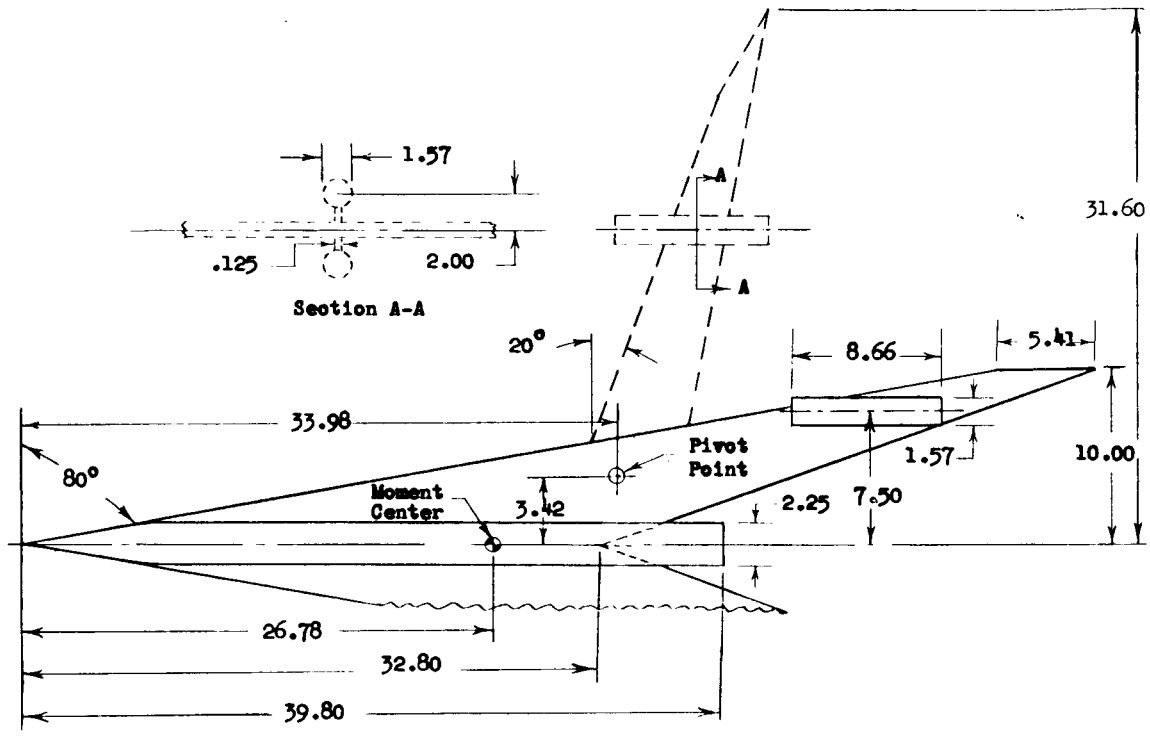

All dimensions in inches.

GEOMETRIC CHARACTERISTICS

Airfoil section normal to leading edge	NACA 63_{10}A014
Camber and twist	None
Aspect ratio:	
For $\Lambda = 20^{\circ}$	10.35
For $\Lambda = 80^{\circ}$	1.05
Area, sq ft:	
For $\Lambda = 20^{\circ}$	2.68
For $\Lambda = 80^{\circ}$	2.65
Reference chord ($\bar{c}$ for $\Lambda = 80^{\circ}$), ft	1.865
Moment reference point	$0.234\bar{c}$

Figure 1.- Drawing of configuration I.

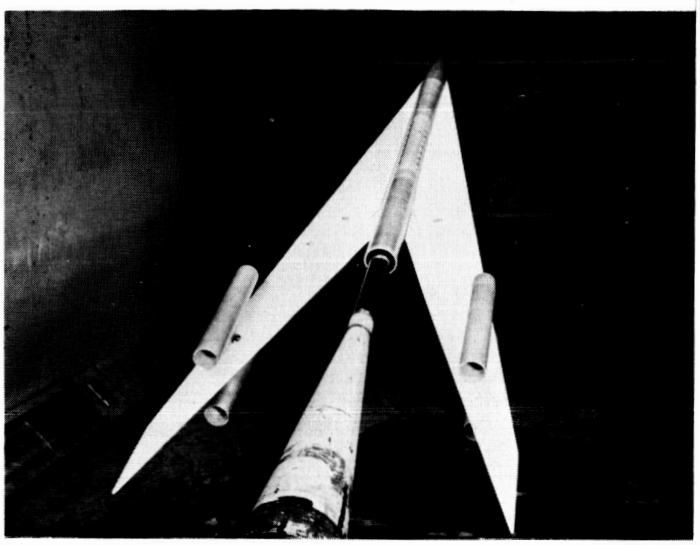

(a) $\Lambda = 80^{\circ}$. L-58-1325a

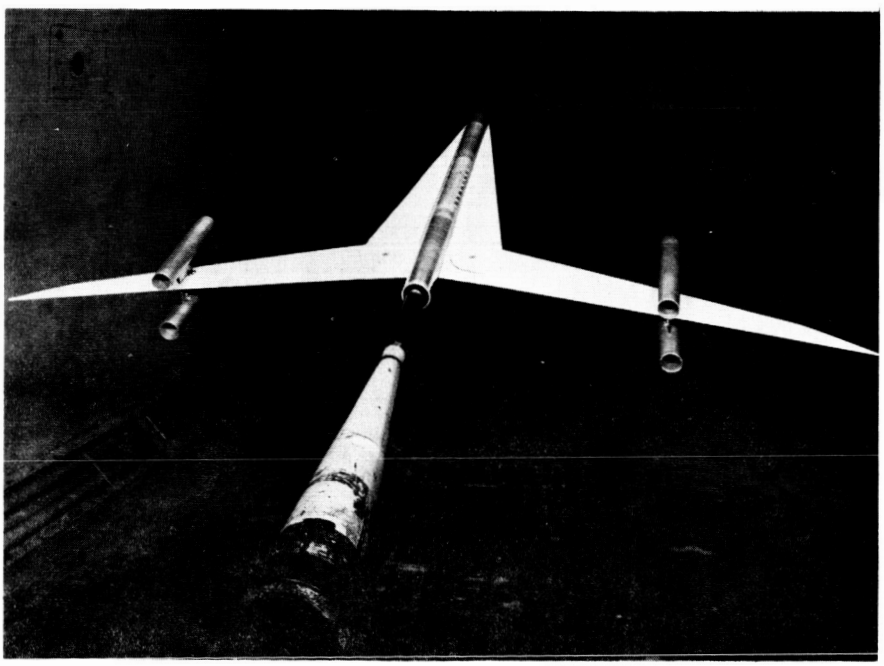

(b) $\Lambda = 20^{\circ}$. L-58-1324a

Figure 2.- Photographs of configuration I.

L-684

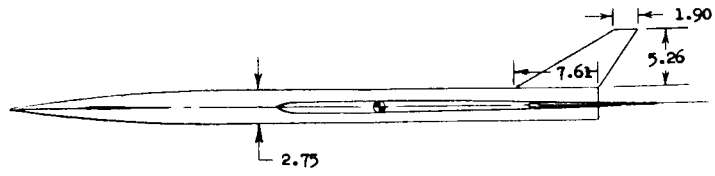

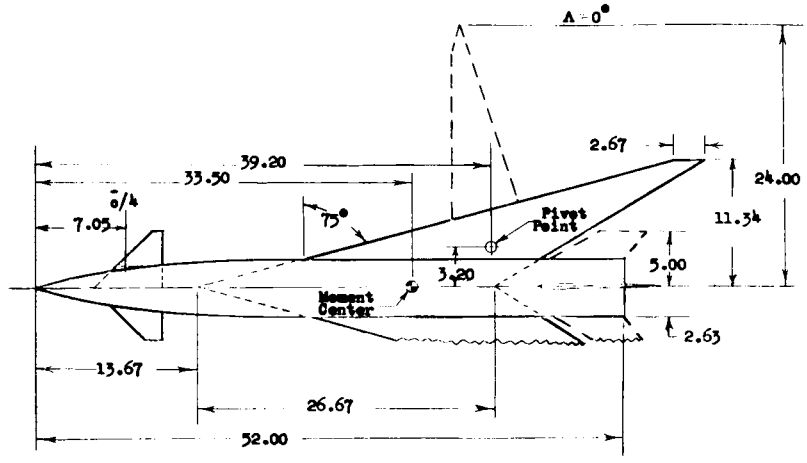

All dimensions in inches.

L-684

GEOMETRIC CHARACTERISTICS

Canard surface:	
Area, sq ft	0.265
Aspect ratio	2.81
Auxiliary tail (folded for $\Lambda = 75^{\circ}$):	
Area, sq ft	0.460
Aspect ratio	1.51
Wing:	
Airfoil section normal to leading edge	NACA 638A007.7
Camber and twist	None
Aspect ratio:	
For $\Lambda = 0^{\circ}$	6.95
For $\Lambda = 75^{\circ}$	1.53
Area, sq ft:	
For $\Lambda = 0^{\circ}$	2.30
For $\Lambda = 75^{\circ}$	2.31
Reference chord ($\bar{c}$ for $\Lambda = 75^{\circ}$), ft	1.50
Moment reference point	$0.25\bar{c}$

Figure 3.- Drawing of configuration II.

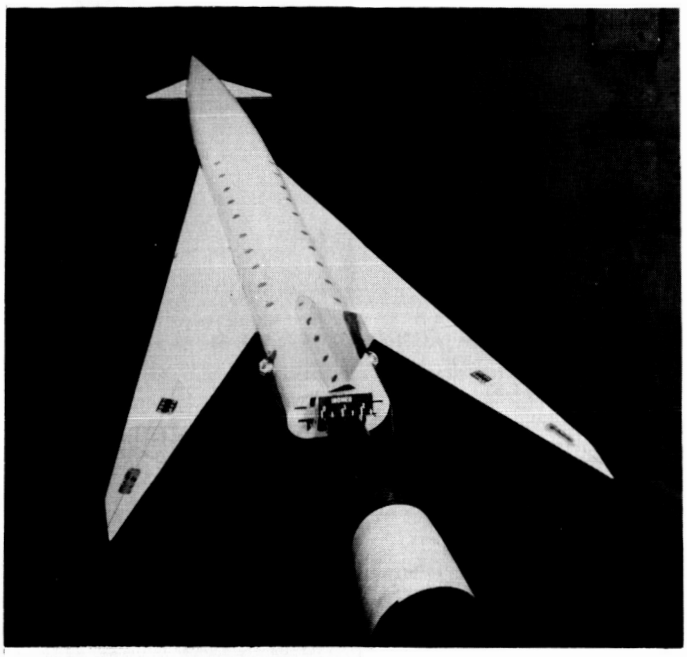

(a) $\Lambda = 75^{\circ}$. L-58-1108a

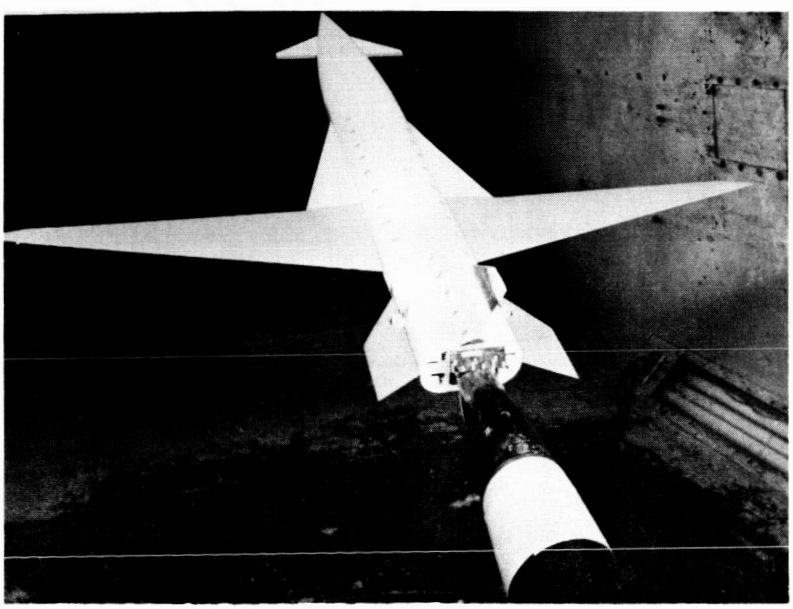

(b) $\Lambda = 0^{\circ}$. L-58-1111a

Figure 4.- Photographs of configuration II.

L-684

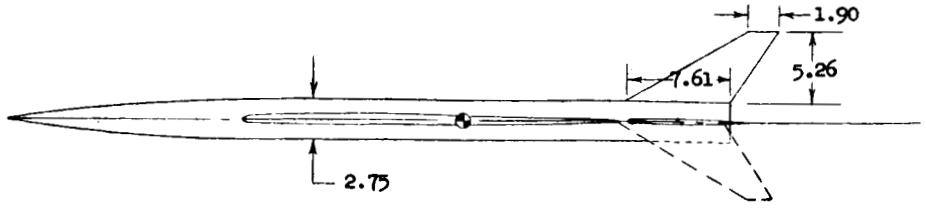

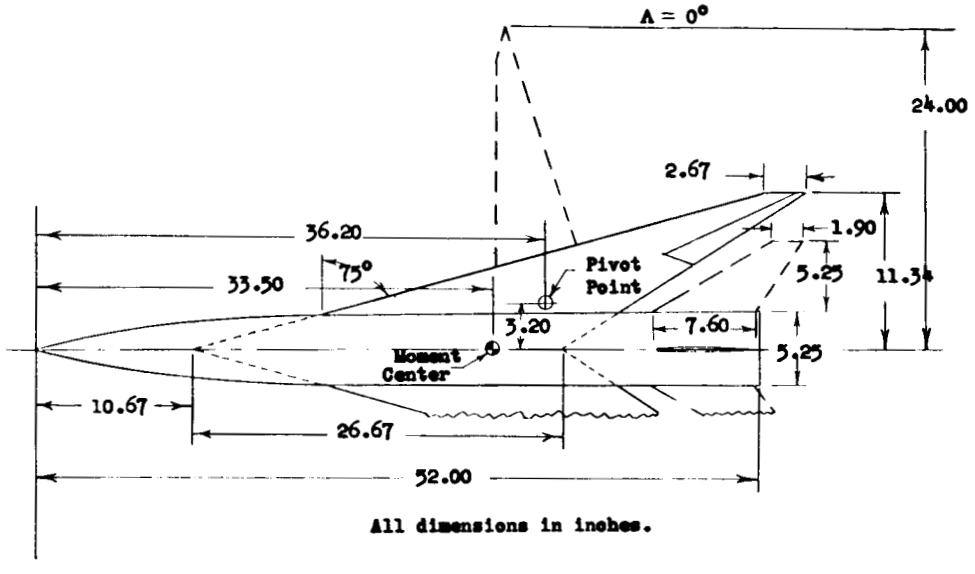

GEOMETRIC CHARACTERISTICS

Horizontal tail (folds for $\Lambda = 75^\circ$):

Area, sq ft	0.69
Aspect ratio	2.50

Wing:

Airfoil section normal to leading edge	NACA 63$_8$A007.7
Camber and twist	None
Aspect ratio:	
For $\Lambda = 0^\circ$	6.95
For $\Lambda = 75^\circ$	1.53
Area, sq ft:	
For $\Lambda = 0^\circ$	2.30
For $\Lambda = 75^\circ$	2.31
Reference chord ($\bar{c}$ for $\Lambda = 75^\circ$), ft	1.50
Moment reference point	$0.404\bar{c}$

Figure 5.- Drawing of configuration III.

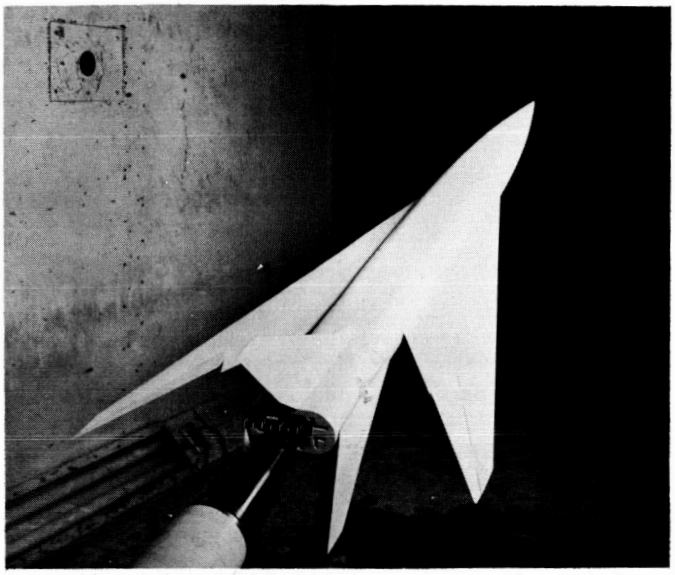

(a) $\Lambda = 75^{\circ}$. L-58-891a

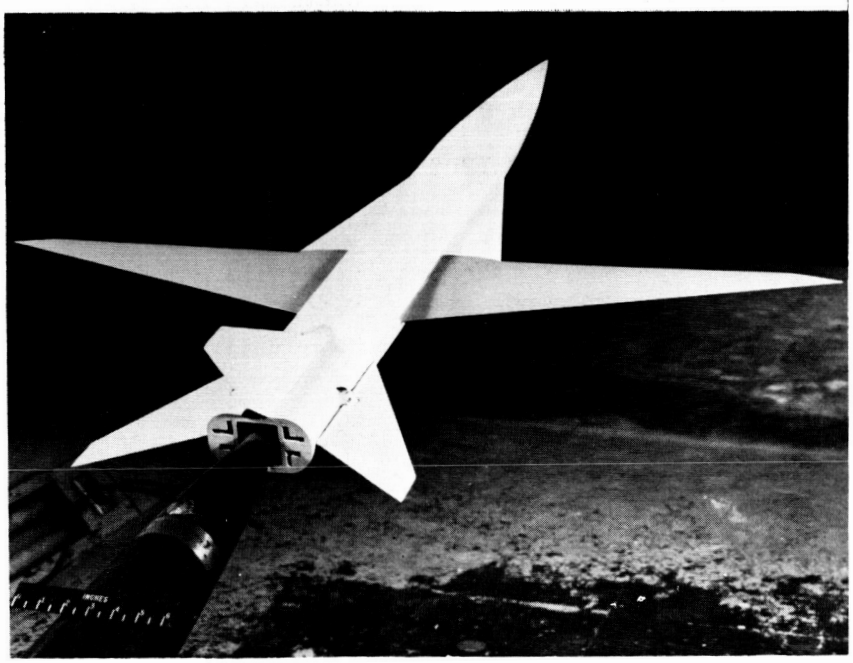

(b) $\Lambda = 0^{\circ}$. L-58-778a

Figure 6.- Photographs of configuration III.

[redacted]

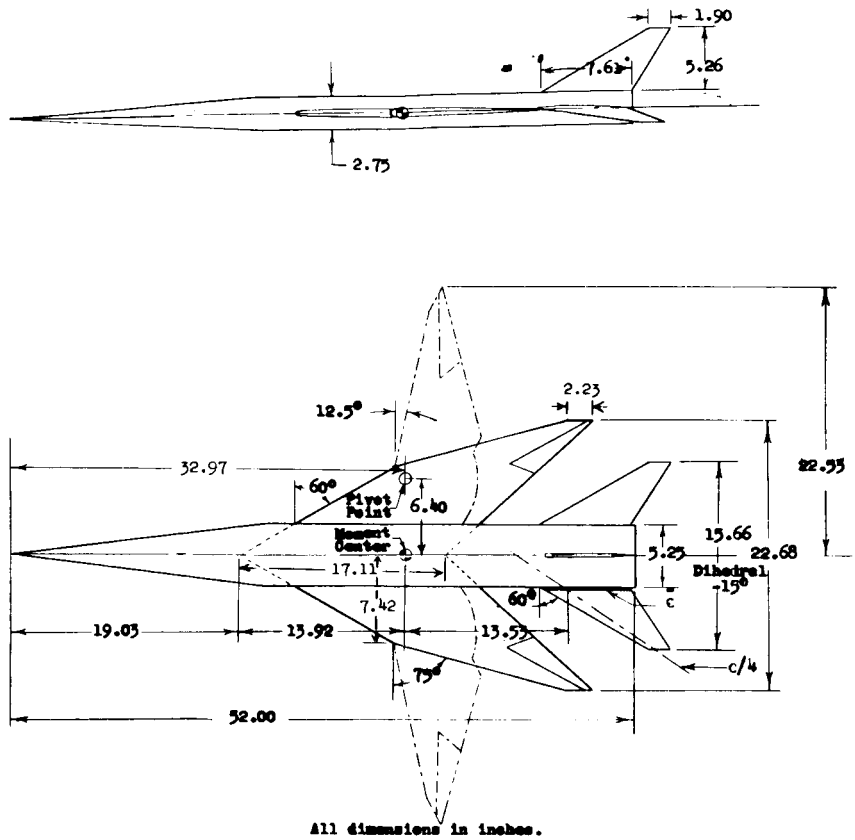

GEOMETRIC CHARACTERISTICS

Horizontal tail (fixed):	
Area, sq ft	0.69
Aspect ratio	2.50
Dihedral, deg	-15°
Wing:	
Airfoil section normal to leading edge	NACA 63$_6$A004.5
Camber and twist	None
Aspect ratio:	
For Λ = 12.5°	6.25
For Λ = 75°	1.88
Area, sq ft:	
For Λ = 12.5°	2.30
For Λ = 75°	1.90
Reference chord ($\bar{c}$ for Λ = 75°), ft	1.14
Moment reference point	0.417$\bar{c}$

Figure 7.- Drawing of configuration IV.

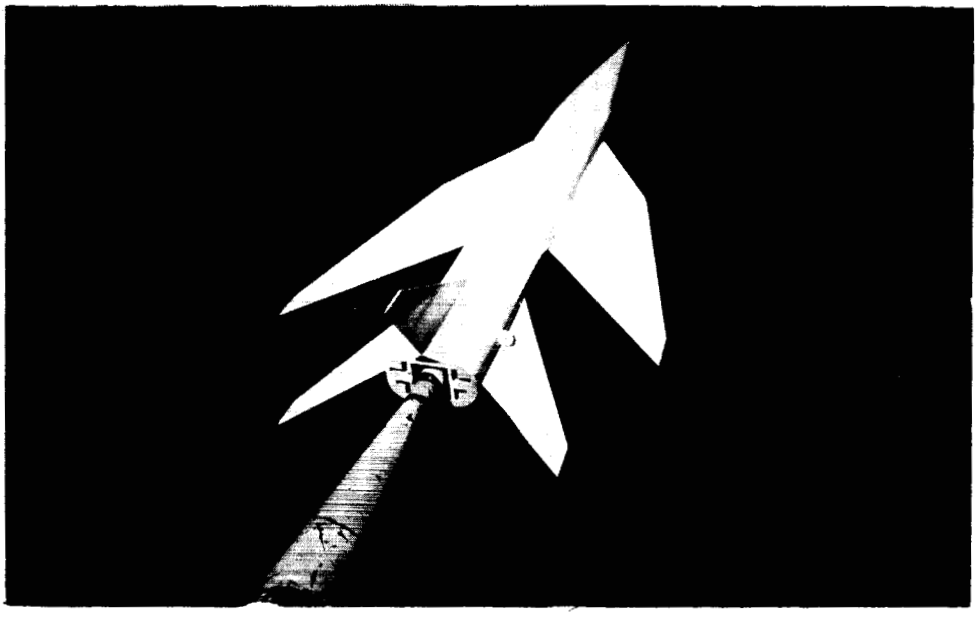

(a) $\Lambda = 75^{\circ}$. L-59-2044

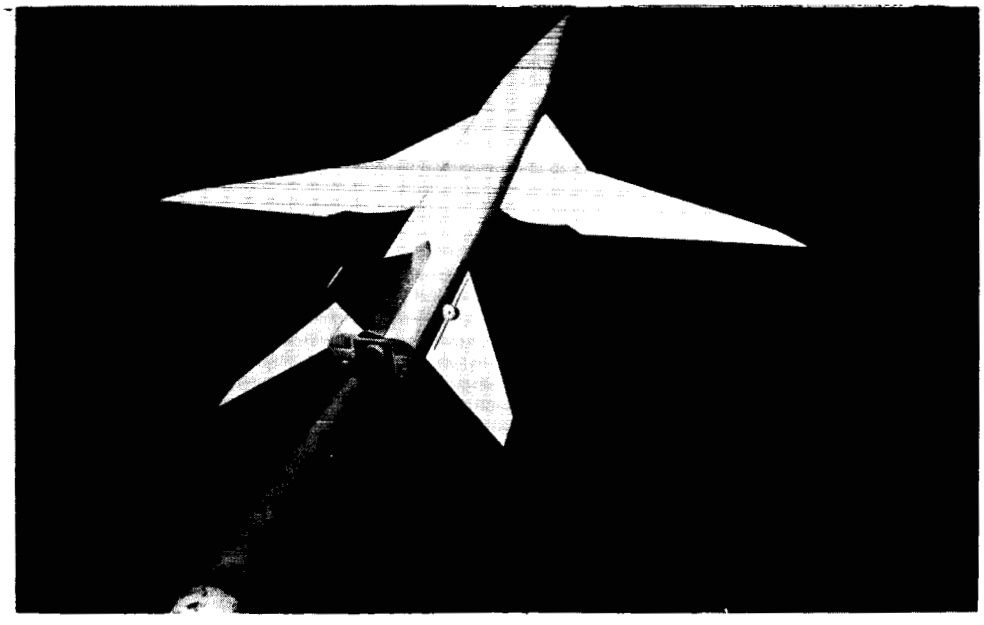

(b) $\Lambda = 12.5^{\circ}$. L-59-2045

Figure 8.- Photographs of configuration IV.

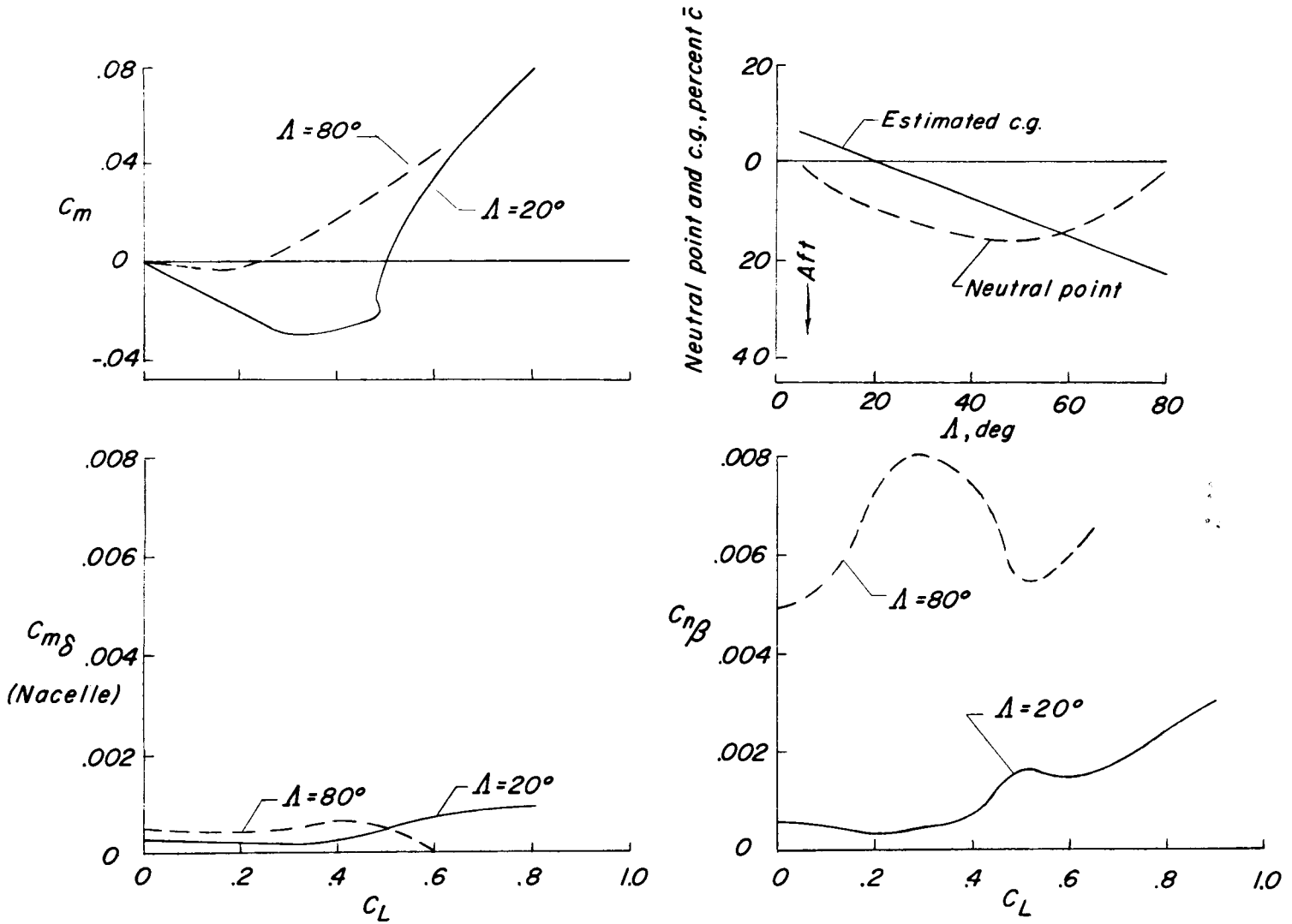

Figure 9.- Summary of characteristics of configuration I at M = 0.25.

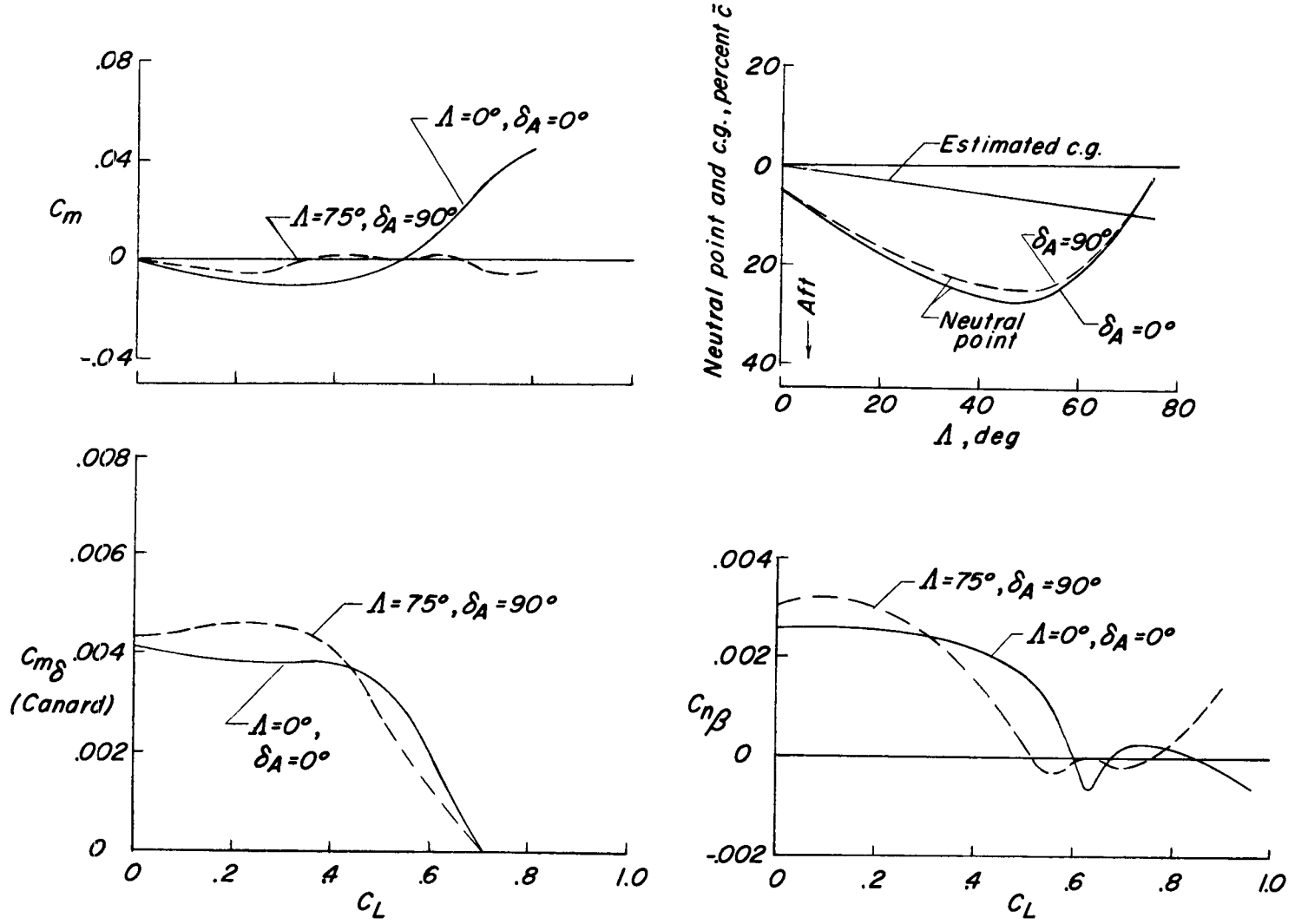

Figure 10.- Summary of characteristics of configuration II at M = 0.25.

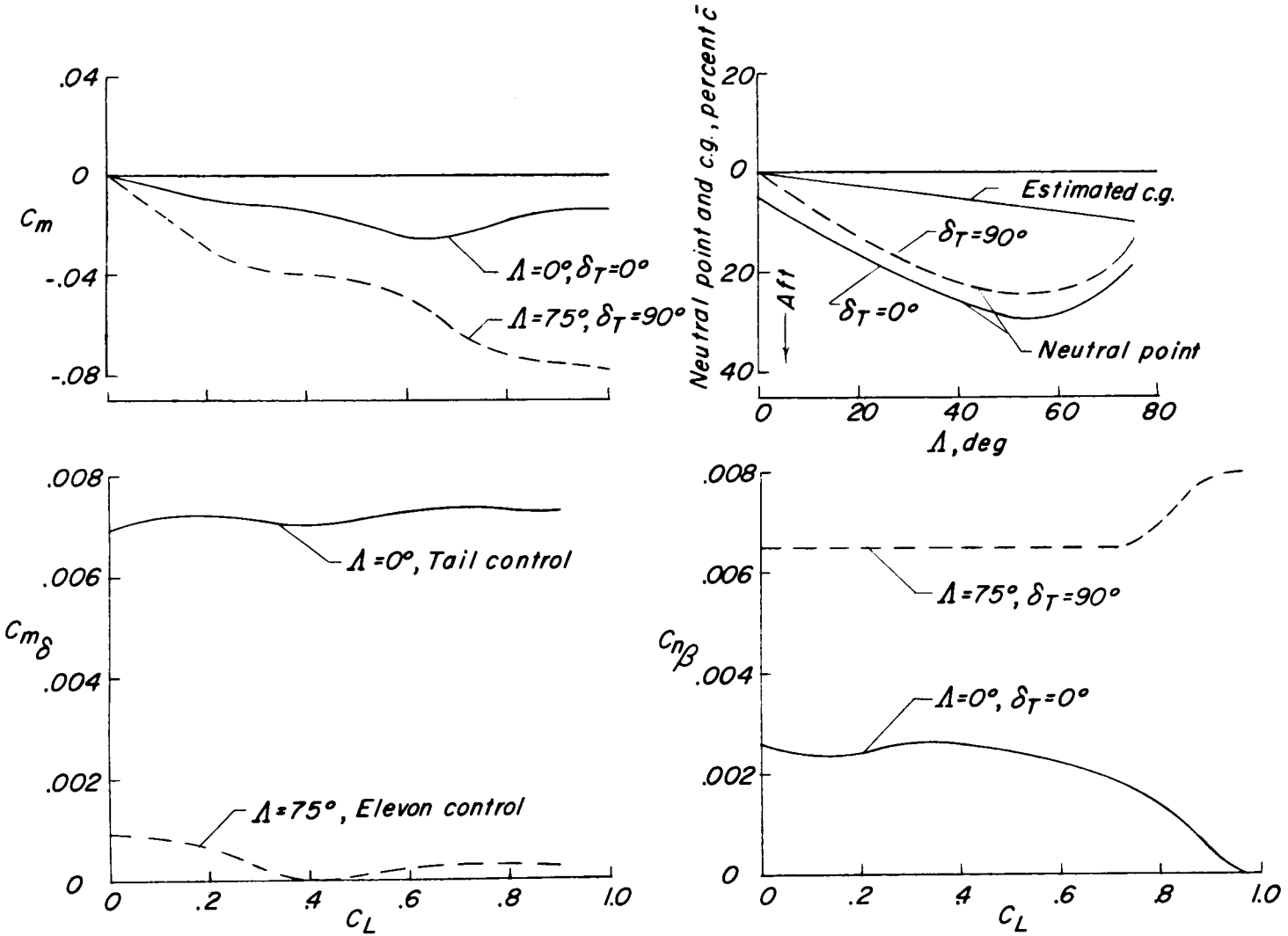

Figure 11.- Summary of characteristics of configuration III at M = 0.25.

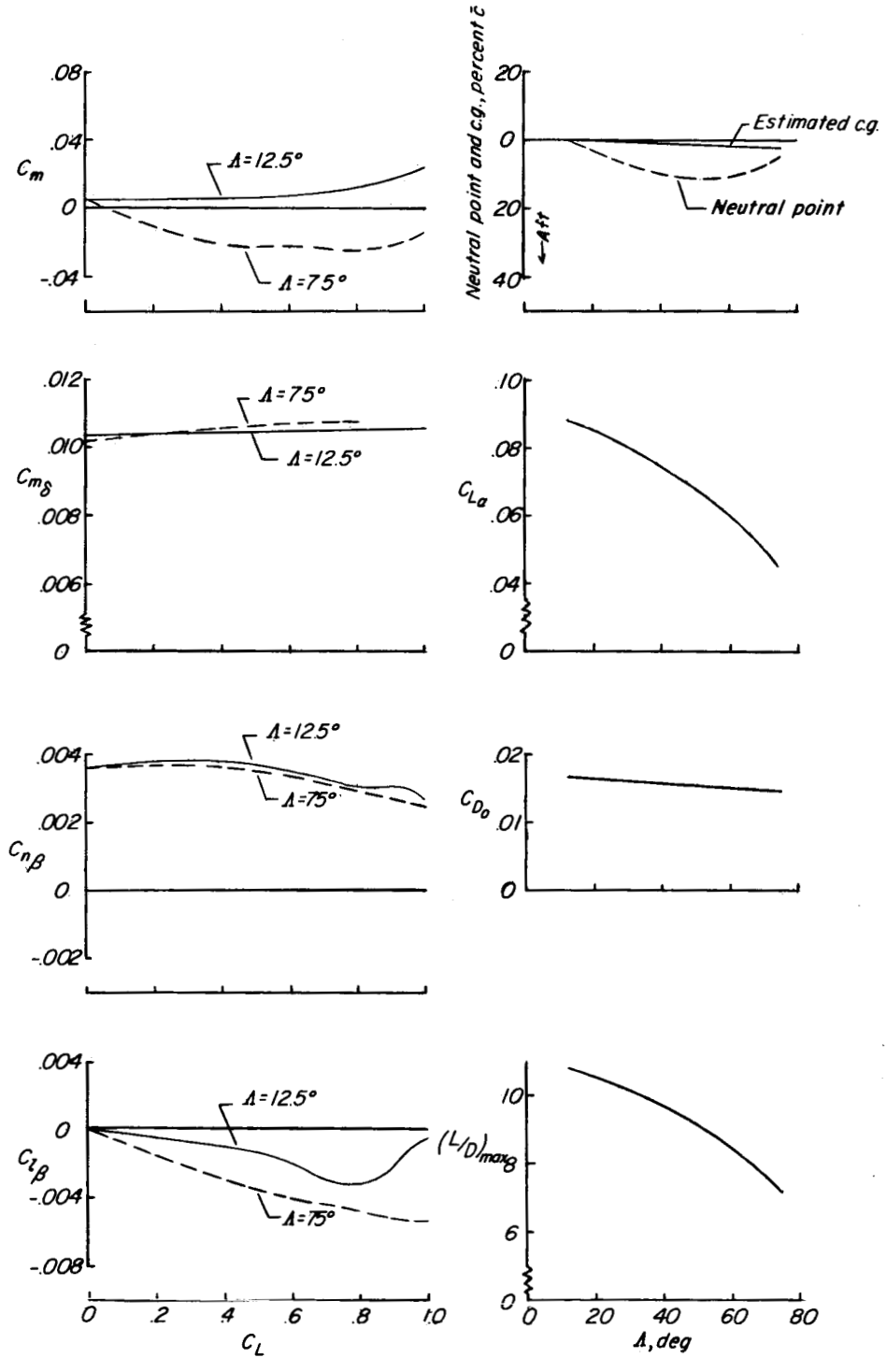

Figure 12.- Summary of characteristics of configuration IV at M = 0.25.

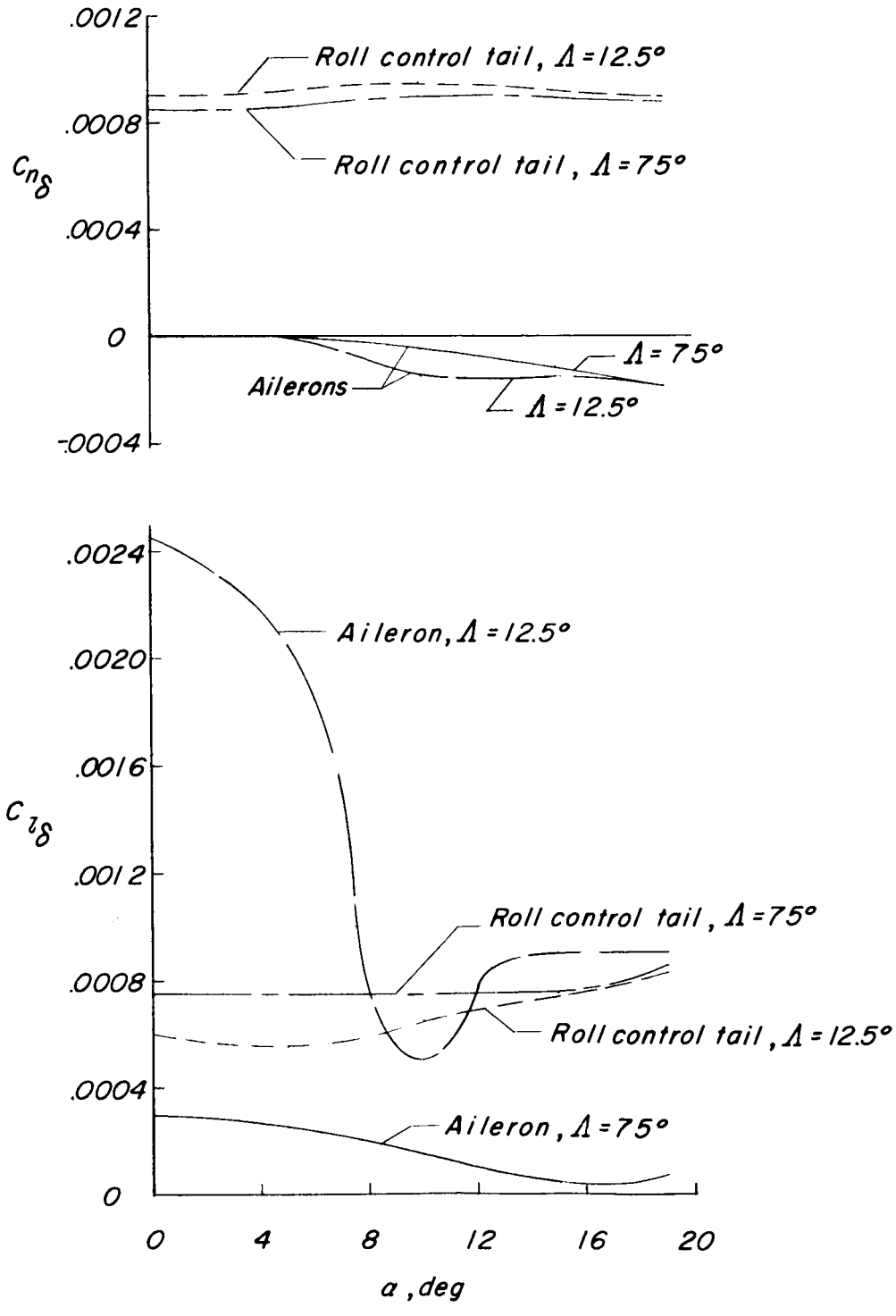

Figure 13.- Lateral control characteristics of configuration IV at M = 0.25.